Phylogeographic patterns driven by river isolations in an island-endemic montane plant

Shaojun Ling[1], Juli Caujapé-Castells[2], Liang Tang[1], and Mingxun Ren[1]

[1]Hainan University
[2]Jardin Botanico Canario "Viera y Clavijo"

March 07, 2024

Abstract

Hainan Island in south China is a key part of the globally important Indo-Burma biodiversity hotspot, while the origin and maintenance of its species richness remains largely unexplored. In this study, we combined nuclear ITS and cpDNA trnL-trnF and ycf1b sequences to evaluate the genetic structure and phylogeographic patterns of the Hainan-endemic Primulina heterotricha (Gesneriaceae). The results showed significant phylogeographic patterns with low within-population genetic diversity and significant genetic differentiation among populations (Fst = 0.708 ± 0.319 and 0.826 ± 0.209 for nrDNA and cpDNA). Three clades were identified with little gene flow (Nm << 1 for nrDNA and cpDNA), which is supported by our STRUCTURE v.2.3.4 analyses. Our analyses detected two vicariance events at c. 0.83 and c. 0.48 Myr, and suggest that these three genetically-separated groups were isolated by two big rivers (Changhua River and Wanglou River), that likely acted as barriers to gene flow. The magnitude of isolation was positively correlated to the size of the rivers, with the greater barrier effect associated with the larger Changhua River. Our results highlight for the first time the critical role of riverine isolation in the patterns of intraspecific evolution of plant populations on Hainan Island.

Original Article

Phylogeographic patterns driven by river isolations in an island-endemic montane plant

Shaojun Ling[1,2], Juli Caujapé-Castells[3], Liang Tang[1,2] and Mingxun Ren[1,2]*

[1]Key Laboratory of Genetics and Germplasm Innovation of Tropical Special Forest Trees and Ornamental Plants (Hainan University), Ministry of Education, Haikou 570228, China

[2]Center for Terrestrial Biodiversity of the South China Sea, Hainan University, Haikou 570228, China

[3]Departamento de Biodiversidad Molecular y Banco de DNA, Jardín Botánico Canario 'Viera y Clavijo' – Unidad Asociada CSIC, Cabildo de Gran Canaria, Camino del Palmeral 15, 35017 Las Palmas de Gran Canaria, Spain

Running title : Phylogeography driven by rivers

*Corresponding author. E-mail: renmx@hainanu.edu.cn**Abstract** Hainan Island in south China is a key part of the globally important Indo-Burma biodiversity hotspot, while the origin and maintenance of its species richness remains largely unexplored. In this study, we combined nuclear ITS and cpDNA *trn* L-*trn* F and*ycf* 1b sequences to evaluate the genetic structure and phylogeographic patterns of the Hainan-endemic *Primulina heterotricha* (Gesneriaceae). The results showed significant phylogeographic patterns with low within-population genetic diversity and significant genetic differentiation among populations ($Fst = 0.708 \pm 0.319$ and 0.826 ± 0.209 for nrDNA and cpDNA). Three clades were identified with little gene flow ($Nm << 1$ for nrDNA and cpDNA), which is supported by our STRUCTURE v.2.3.4 analyses. Our analyses detected

two vicariance events at *c.* 0.83 and*c* . 0.48 Myr, and suggest that these three genetically-separated groups were isolated by two big rivers (Changhua River and Wanglou River), that likely acted as barriers to gene flow. The magnitude of isolation was positively correlated to the size of the rivers, with the greater barrier effect associated with the larger Changhua River. Our results highlight for the first time the critical role of riverine isolation in the patterns of intraspecific evolution of plant populations on Hainan Island.

KEYWORDS Biogeography, Changhua River, Isolation, Phylogeographic patterns, Hainan Island

1 INTRODUCTION

Geographical isolation refers to a situation where populations become separated by physical barriers such as islands and mountains, and has long been considered as a key driving force in speciation (MacArthur & Wilson, 1967; Li et al., 2011; Robin et al., 2015). Geographical barriers can fragment distribution ranges and gene flow dynamics between different sides of the barriers, thereby allowing the increase in population differentiation. As a result, populations become fragmented and genetically isolated and, in some cases, new species may evolve (Crimmins et al., 2011; Li et al., 2011; Robin et al., 2015; Demenou et al., 2016). The knowledge of such processes is crucial for gaining insight into the origins and evolution of biodiversity, but also useful for formulating biodiversity conservation strategies. Consequently, the identification of geographic barriers using genetic data is increasingly emphasized in modern biodiversity conservation studies (Li et al. , 2011; Robin et al. , 2015; Tan et al. , 2020).

Hainan Island in south China harbors *c.* 4800 seed plant taxa in total and about 500 endemics (Francisco-Ortega et al. , 2010a, b; Yang, 2013), and is a distinctive part of the globally important Indo-Burma biodiversity hotspot (Myers et al. , 2000). Notably, the richest biodiversity and 80% of the endemic species occur in the south-central mountains of the island (Yu et al. , 2001; Francisco-Ortega et al. , 2010a, b), which are largely located within Hainan Tropical Rainforest National Park. Home to rich tropical plant species, this Park is an important natural gene pool for the entire globe. However, several large rivers, mountains and valleys cause a pronounced geographical fragmentation in this region (Ling et al., 2017a, b; Li et al., 2020), with potentially negative effects on ecosystem integrity and the biodiversity conservation of the Park. Such patterns offer opportunities to study the mechanisms underlying evolutionary species diversification in the island, which involves both isolation by the sea and by riverine and mountainous barriers.

The family Gesneriaceae in Hainan Island is notable for its extremely high species endemism (Wei, 2010; Ling et al., 2017a, 2017b). Fourteen genera and 25 species of Gesneriaceae are currently found on the island, including two endemic genera and nine endemic species (Li & Wang, 2005; Yang, 2013; Ling et al., 2017a, 2020b). The species endemism proportion of Hainan Gesneriaceae is 30%, a great value similar to that of the nearby Guangxi Province (Ling et al., 2017b), long believed to be the species distribution and endemism centre of Gesneriaceae in SW China due to its widespread limestone landscapes (Li & Wang, 2005; Wei et al., 2004; Wei, 2010). All these Hainan endemics are found on crown lineages (Ling et al., 2017b), suggesting a recent origin (Ling et al., 2017b, 2020a). However, the mechanisms and processes underlying speciation patterns of these narrow endemics have received little attention.

In this investigation, we examine the influence of rivers and mountains on the genetic divergence and phylogeographic patterns in the Hainan-endemic *Primulina heterotricha* (Merr.) Y.Dong & Yin Z.Wang (Gesneriaceae) using both nuclear and chloroplast DNA sequences. This study addresses three specific questions to test if the geographical isolation of populations by rivers and valleys on the island were determinant to the speciation, distribution and genetic diversification of *P. heterotricha* : (1) What is the genetic and phylogeographic structure of *P. heterotricha* populations? (2) Can these patterns be associated with any geographic barriers? (3) Did these barriers play a role in the speciation and adaptation history of this montane plant?

2 MATERIAL AND METHODS

2.1 Plant material

Primulina heterotricha is an endemic perennial shrub with thick rhizome that inhabits limestone or granite streamsides in forested valleys, widely distributed in south-central mountain systems of Hainan Island (Li

& Wang, 2005; Wei, 2010; Yang, 2013). Its populations display a limited range of morphological diversity including irregular pale yellow or purple corollas. The plant has zygomorphic tubular flowers which are pollinated by several insects, especially *Glossamegilla malaccensis* (Anthophoridae) Friese and *G. yunnanensis* Wu (Anthophoridae)(Ling, 2017). The capsule is erect with small brown and fusiform shaped seeds, indicating a weak dispersal capability with no wind- or animal-mediated dispersal features.

2.2 Sample collection and laboratory procedures

From 2015 to 2017, we conducted a thorough sampling across the known distribution range in the south-central mountain systems of Hainan Island and we collected 217 leaf samples from 10 populations of *P. heterotricha* (Table 1, Figure 1). Each sampled leaf was dried in a separate plastic bag containing 20 to 30 g of silica gel. We collected two individuals with flowers and fruits as representative herbarium vouchers, and these have been deposited in HUTB, under accession numbers *Ling & Ren 2016091902* and *Ling & Ren 2016091501* . Total genomic DNA for each sample was extracted using the CTAB method (Doyle & Doyle, 1987), and served as the template for the polymerase chain reaction. DNA quality and quantity on 0.8% agarose gels stained with 2.5 μl Goldview (Aidlab Biotechnologies Co., Ltd) was detected by AL2000 DNA maker (Aidlab Biotechnologies Co., Ltd) in DTU-48 spedtrophotometer (Hangzhou Miu Instruments Co., Ltd, China).

One nuclear ribosomal DNA (nrDNA) sequence, the ITS region comprising spacer 1, the 5.8S gene and spacer 2 (White et al. , 1990) and two chloroplast DNA (cpDNA) intron-spacer region *trn* L-*trn* F (Taberlet et al. , 1991) and *ycf* 1b (Dong et al. , 2015) were used in this study (Table 2). PCR reactions were set up in a volume of 25 μl composed of 20 μl ddH_2O, 2.5 μl 10×Buffer, 0.5 μl 10 mM dNTPs, 0.5 μl each 5 μM primer, 0.5 μl DNA template and 0.5 μl 5 U/μl Taq polymerase (Aidlab Biotechnologies Co., Ltd). The PCR reactions were carried out on the 2720 Thermal cycler (Applied Biosystems by Life Technologies, made in Singapore) and Veriti 96-Well Thermal Cycler (Applied Biosystems by Life Technologies, made in Singapore). The PCR program for ITS1/2 and *trn* L-*trn* F was designed to an initial denaturation at 94 ºC 5 min, followed by 35 cycles of 1 min at 94 ºC, 1 min at 55 ºC, 1 min at 72 ºC, and with a final extension of 10 min at 72 ºC. Amplification of *ycf* 1b used the following protocol: 4 min at 94 ºC, 35 cycles of 30 s at 94 ºC, 40 s at 58 ºC, and 1 min at 72 ºC, ending with 10 min at 72 ºC. All the PCR products were verified by cataphoresis. The amplicons were sequenced by an ABI 3730 DNA Analyzer based on the BigDye Terminator Cycle Sequencing Ready Kit (Applied Biosystems, Foster City, CA) in BGI (Beijing Genomics institution).

2.3 Genetic diversity

The chromatograms from both directions of the ITS1/2 and cpDNA sequences were edited with the software BioEdit (Hall, 1999) for base confirmation and contiguous sequences editing. The sequences were manually aligned where necessary using MEGA v.6.5 (Kumar et al. , 2008). All sequences have been deposited in Genbank. The two non-coding cpDNA sequences were assembled as a single locus by SequenceMatrix v.1.7.8 (Vaidya et al., 2011), and a Partition Homogeneity Test (PHT) vs the ITS sequences was carried out with PAUP* v. 4.0a164 (Swofford, 2002). Since the test resulted in the non-homogeneity of both matrices, we analysed the geographic distribution of ribotypes/chlorotypes for nrITS and cpDNA sequences separately.

DNASP v. 6.12.01 (Rozas et al. , 2017) was used to compute the number of ribotype/chlorotype (h), haplotype diversity (Hd) within populations, polymorphic sites (S), nucleotide diversity (π), average number of nucleotide difference (K).

2.4 Population structure analysis

To explore the phylogeographic structure of ribotypes/chlorotypes, gene diversity within populations (h_S), gene diversity (h_T), index of gene diversity of total populations (N_{ST}) and index of genetic differentiation between populations (G_{ST}) were calculated using the HAPLONST (Pons & Petit, 1996). This software was also used to compute the test statistic U that compares the values of N_{ST} and G_{ST} , which indicates the presence of phylogeographic structure ifN_{ST} is higher than G_{ST}(Pons & Petit, 1996).

Since the cpDNA is maternally inherited in *Primulina* , there is no recombination among loci and structure analysis makes no sense for such dataset. Population structure of nrDNA sequences was inferred using the Bayesian clustering procedure implemented in the software STRUCTURE v.2.3.4 (Evanno et al. , 2005), that identifies the most probable number (K) of genetic clusters of origin of the sampled individuals, and assigns individuals to clusters. We used Markov Chain Monte Carlo (MCMC) iterations as implemented in the software to explore the parameter space considering individual memberships to the Kclusters, ranging from $K = 1$ (null hypothesis of panmixia) to$K = 10$ (the total number of populations sampled). Three independent runs were performed with an admixture model at 10^5 MCMC iterations and a 10^5burn-in period. The most likely number of population groups (K , indicating the number of true clusters in the data) and the model values (^{K})$according to the second-order rate of Change of cluster$K$that best fit the data was calculated in Structure Harvester (Earl\&von Holdt, 2012). The graphica$ //clumpak.tau.ac.il/index.html).

*The genetic differentiation (*Fst *) and gene flow (*Nm *) between populations and among different regions for nrDNA and cpDNA sequences separately. An Analysis of Molecular Variance (AMOVA) was conducted on nrDNA and cpDNA sequences separately to test genetic differentiation within populations, among regions and among populations within regions using GENALEX v. 6.503 (Peakall & Smouse, 2012). To test whether there was local genetic variation attributable to isolation by distance (IBD), Nei's genetic distances (Nei, 1973) calculated with by MEGA v. 6.5 and geographic distances (in km) between all pair-wise combinations of the ten populations sampled were subjected to a Mantel test (Mantel, 1967) in GENALEX v. 6.503. The genealogical relationships between ribotypes/chlorotypes were inferred from the Median-Joining network (MJ) of NETWORK v4.6.1.0 (http://www.fluxus-Engineering.com/). In order to identify and quantify potential genetic discontinuities and biogeographic boundaries between populations from both nrITS and cpDNA datasets, we calculated the Monmonier's maximum-difference algorithm in Barrier v.2.2 (Manni et al., 2004). The robustness of these barriers was assessed by bootstrap, as in the Barrier v.2.2.*

2.5 Phylogenetic relationships of ribotypes

Phylogenetic relationships for the identified ribotypes were reconstructed with Maximum Likelihood (ML) and Bayesian Inference (BI) using MEGA v.6.5 (Kumar et al. , 2008) and MrBayes v.3.2.6 (Ronquist et al. , 2012). Primulina pteropoda *(W.T.Wang) Yan Liu was used as outgroup with sequences of nrDNA (Gao et al. , 2015, Genbank with accession number DQ872827).*

We inferred the optimal model of nucleotide substitution using MrModeltest 2.3 (Nylander, 2004), based on the AIC (Akaike Information Criteria) (Akaike, 1981). The most suitable model (GTR+I+G) was used in both Maximum Likelihood (ML) and Bayesian inference (BI) analysis. ML analysis was conducted using MEGA v.6.5 with the optimal substitution model, and 1000 bootstrap (BS) replicates were carried out to assess the support of the resulting groups. BI analysis was conducted using MrBayes v.3.2.6. The Markov Chain Monte Carlo (MCMC) was run for 10 million generations, sampling every 10,000 generations across four independent Bayesian runs. The first 2500 trees (25% of total trees) were discarded as burn-in, and the remaining trees were summarized in a 50% majority-rule consensus tree with the posterior probabilities (PP). Chain convergence was assessed by checking the effective sample size (ESS) that was bigger than 200 for each parameter in Tracer v.1.6 (Rambaut &+' Drummond, 2007), and the length and PP of each branch were visualized by FIGTREE v.1.4.2 (Rambaut, 2009).

2.6 Molecular dating of chlorotypes and population historical dynamics

*Divergence dating of the chlorotypes in a Bayesian framework was performed in BEAST v.1.7.5 (Drummond et al. , 2012). Owing to the absence of fossil records of Gesneriaceae with known ages, we used*P. pteropoda *(with an estimated age of* c. *1.31 Myr; Gao et al. , 2015; Genbank accession number KF498219) to calibrate a molecular clock, on the grounds that it has the closest phylogenetic relationship with* P. heterotricha *(Gao et al. , 2015). Four independent Markov Chain Monte Carlo (MCMC) runs were analyzed for 80 million generations and sampled every 1000 steps with the nucleotide substitution model GTR+I+G, as selected by MRMODELTEST 2.3 (Nylander, 2004) based on the Akaike Information Criteria (AIC). The Yule speciation*

tree priors and the relaxed clock model with an uncorrelated lognormal distribution were followed. The resulting trees from the four runs were combined by LOGCOMBINER (Bouckaert et al. , 2014), discarding the first 25% of generations as burn-in. We specified a normal distribution with standard deviation of one million years for all the time priors. TRACER 1.5 (Rambaut & Drummond, 2007) was used to access the chain convergence and ensuring ESS values was well above 200. The maximum clade credibility (MCC) tree was summed up using TREEANNPTATOR in the BEAST package (Bouckaert et al. , 2014). The averages and PP of age estimates were visualized by FIGTREE v.1.4.2 (Rambaut, 2009).

The probable ancestral biogeographical scenarios in the phylogeny of P. heterotricha *chlorotypes were reconstructed separately by a Statistical Dispersal-Vicariance Analysis (S-DIVA) by using the S-DIVA (Yu* et al. *, 2010), which is parsimony-based and favours vicariance events without any prior assumptions about area relation (Yu et al. , 2010). We chose to be cautious in our definition of regions, and arranged three areas based on the geographic barriers and contiguities: (1) NW-Northwest of Changhua River, including the populations BW, YJ, EX, WX and YG; (2) SE-Southeast of Changhua River, including the populations WZ, QX, XA and QL; (3) SW-Southwest of Changhua River, consisting only of the population JF. The chlorotype trees for S-DIVA analysis were generated in BEAST v.1.7.5, including the outgroup* P. pteropoda *(see above).*

In order to detect possible recent range expansions, Tajima's D *(Tajima, 1989) and Fu's* F *s (Fu, 1997) were calculated for testing the deviations from the null hypothesis of constant population size and neutral evolution for each DNA fragment, pairwise mismatch distribution and neutrality tests for all populations and clades (NW, SE and SW) were conducted in DNASP v. 6.12.01 based on nrITS and cpDNA separately. These tests show a unimodal shape in the mismatch distribution of populations that experienced historical expansion.*

3 Results

3.1 nrITS and cpDNA dataset acquisition and assessment

Twelve ITS ribotypes were identified based on 16 variable nucleotide sites. The ITS1/2 length was 701 bp, nucleotide diversity (π) was 0.00390, the average number of nucleotide difference (K) was 2.681, and haplotype diversity (Hd) was 0.810 (Table 2). The geographical distribution of ribotypes showed that only a few ribotypes were shared across the species distribution range, whereas most of them were private to a single population (Table 1, Figure 1).

The two cpDNA sequences used contained 50 polymorphic sites, and yielded 19 chlorotypes. Nucleotide diversity (π) was 0.00860, average number of nucleotide difference (K) was 11.634, haplotype diversity (Hd) was 0.919 (Table 2). All chlorotypes were exclusive to a single or a group of neighbouring populations (Table 1, Figure 1). The total length of the combined chloroplast alignments was 1404 bp (730 bp and 674 bp in size for trn *L-*trn *F and* ycf *1b, respectively), a congruency test implied a high level of homogeneity of the two chloroplast sequences (*P *> 0.5) and a striking non-homogeneity between nrDNA and cpDNA (*P *< 0.5). Ribotype and chlorotype diversities (Hd) of the 10 sampled populations ranged from 0 to 0.586 and 0 to 0.711 respectively (Table 1).*

3.2 Phylogeographical patterns and population genetic structure

Overall ribotype and chlorotype diversities (h_T *) were 0.908 and 0.970 respectively, and within-population ribotype and chlorotype diversity (*h_S *) were 0.181 and 0.228 (Table 2). Remarkable population differentiation was detected, with a*G_{ST} *= 0.801 and 0.765 and*N_{ST} *= 0.855 and 0.833. The test statistic*U *resulted in significant divergence between*N_{ST} *and* G_{ST}*(*N_{ST} ¿ G_{ST} *,* P *¡ 0.05), showing a significant phylogeographical patterns of* P. heterotricha *in Hainan Island. The 10 populations of* P. heterotricha *clustered into three major groups according to the STRUCTURE analysis (Figure 4), the likelihood of the nrDNA dataset was also the highest when samples were clustered into three lineages (K=3, Figure S2).*

*The nrDNA and the cpDNA sequences respectively estimated an among-population genetic differentiation (*Fst *) of 0.708 ± 0.319 and 0.826 ± 0.209, gene flow level (*Nm *) of 1.44 ± 3.94 and 0.25 ± 0.73, the majority* Nm *values were less than one (Table 3). Furthermore, the estimated* Nm *of among-region was 0.40 between NW and SE, 0.10 between SE and SW and 0.04 between NW and SW for nrDNA sequences, and*

0.41, 0.07, 0.07 for cpDNA sequences. According to the AMOVA, 72% and 55% of genetic variation among the three regions was respectively attributable to the nrITS and cpDNA differentiation (respectively 17% and 33% among populations, and 11% and 12% within populations, Table 4).

The Mantel tests showed a low but highly significant positive correlation between genetic and geographical distance matrices (respective R^2 values of 0.2544 ($P < 0.001$*) and 0.1479 (*$P < 0.001$*), Figure S1), indicating a slight IBD. The BARRIER analyses suggested two strong barriers to gene flow among the populations of* P. heterotricha *(Figure 5); one of them separated the NW and SW populations (red line, 93% BS), and the other separated the SE populations from the other (green lines, 90% BS). We detected a third, weaker barrier (blue line with BS below 80%) that separated of populations WZ and QX with XA and QL based on the nrITS dataset.*

3.3 Phylogeny of ribotypes

Bayesian inference (BI) and Maximun likelihood (ML) trees separated the 12 ribotypes into three different monophyletic lineages with high PP/BS values. These correspond to populations in the NW, the SE and the SW (Figure 2A). Consistently, the phylogenetic tree (Figure 2B) also showed three independent and well-supported clades.

3.4 Molecular dating of cpDNA and demographic history

The BEAST-derived chronogram of 19 chlorotypes was supported by maximum PP, and revealed three diverging genetic lineages (Figure 3A), which correspond to the NW, SE and SW clades revealed by the chlorotype Median-Joining network (Figure 3B). The time-calibrated phylogenetic tree placed the split of P. heterotricha *at* c. *0.83 Myr (Figure 3A). The splitting time of the remaining chlorotypes from clades NW and SE was estimated at around 0.48 Myr, roughly at the end of early Pleistocene, and most other chlorotypes were dated between* c.*0.26-0.05 Myr (Figure 3). And two vicariance events were detected among three clades, first events gave rise to the genetic split in SW and the rest clades, second events offered opportunity to the genetic divergence in SE and NW clades (Figure S3).*

The results of Tajima's D *test and Fu's* Fs *test were presented in Table 2 with the associated simulated* P *-values. The values for* D *was negative and* Fs *was positive for nrDNA sequences (*$D = -0.00585$*,* $P > 0.10$*;* $Fs = 0.538$*,* $P = 0.132$*), but all were positive for cpDNA sequences (*$D = 0.98381$*,* $P > 0.10$*;* $Fs = 9.119$*,*$P < 0.01$*) (Table 2), indicating an insignificant less and excess of rare nucleotide site variants for nrDNA and cpDNA sequences separately compared to the expectation under a neutral model of evolution, and an significant excess of rare haplotypes for nrDNA and cpDNA sequences over what would be excepted under neutrality. The Hierarchical mismatch analysis showed the distributions of differences for all populations, clade NW, SE and SW were ragged or multimodal (Figure S4), which rejected the hypothesis of demographic population expansion of these population clades.*

4 DISSCUSION

4.1 Phylogeographical patterns driven by river isolation

*Through the examination of the ribotypes and chlorotypes of 217 individuals from 10 populations of the Hainan-endemic herbaceous*P. heterotricha *in the south-central mountain system of Hainan Island, low within-population genetic diversity and high genetic differentiation (*Fst *) among populations were revealed (Figure 1). There was a significant phylogeographical structure and AMOVA showed high genetic variation mainly from inter-regions (Table 4). Three clades NW, SE and SW have evolved in prolonged isolation, as intimated by bayesian analysis (Figure 3), which is supported by results of STRUCTURE v.2.3.4. (Figure 4), and low gene flow (*Nm *) among regions were detected. Two main genetic barriers were identified based on Monmonier's algorithm (Figure 5), which spatially concordant with the Changhua River and Wanglou River in south-central mountains system of Hainan Island (Figure 2, 3 and 4).*

The average population genetic divergence detected in P. heterotricha *is high overall (*$G_{ST} = 0.801$ *and 0.765 for nrITS and cpDNA gene respectively), considering that genetic differentiation among populations*

turns to be stronger where $G_{ST} > 0.25$ *(Buso et al. , 1998).* Primulina heterotricha *grows widely in rocky streamsides of forest valleys and humid or arid limestone and granites habitat, which are widespread in south-central Hainan Island. Yet, there was a slight IBD, although pollen or seed dispersal is very limited among most populations (*Nm << *1, Table 3) owing to the discussed isolation effect of Changhua River, and the lack of adaptation to long-range seed dispersal. Furthermore, the distribution of effective pollinators (genus* Glossamegilla *) is interrupted easily by rivers and mountains, and it even shows altitudinal differences within the same mountain system (Zhong et al. , 2014).*

Geographic discontinuities are indeed a significant factor for population differentiation through weakening or blocking gene flow (Slatkin, 1985), and their impacts apparently have driven regional genetic differentiation within P. heterotricha *populations. These results are in line with previous studies in other groups, showing that the geographic barrier associated with the course of Changhua River may have stimulated lineage diversification. Two examples are the multiple intra-specific genetic lineages detected in the endemic species*Metapetrocosmea peltata *(Merr. et Chun) W. T. Wang (Gesneriaceae) and genus* Oreocharis *(Gesneriaceae), which also presented a strong phylogeographical population structures (Li et al. , 2020; Ling et al. , 2020a).*

The major role of mountains and valleys in the origins and evolution of plants has been widely reported in the Andes (Antonelli et al., 2009; Pennington et al. , 2010), Ghats (Robin et al. , 2015) and Hengduan Mountain (Liu et al. , 2013). And similar results of genetic structure associated with sharp geographical discontinuities have been reported in many Asian plants and animals. Regarding other families and phyla, Myricaria laxiflora *(Franch.) P.Y. Zhang et Y.J. Zhang (Tamaricaceae) in the Three Gorges mountain region (Liu et al. , 2009),* Taxus wallichiana *Zucc. (Taxaceae) in the Himalaya-Hengduan Mountains region (Liu et al. , 2013), and several endemic montane birds from the Western Ghats (Robin et al. , 2015), all showed nested genetic patterns across complex mountain system isolated by valleys or rivers. The ensuing gene flow limitation, genetic drift enhancement and possibly natural selection, can likely have induced the genetic structure detected, that may in the long term lead to reproductive isolation and speciation.*

*Our genetic data pinpoint the lower Changhua River as the stronger gene-flow barrier between NW and SW clades (93% bootstrap) with minimum*Nm = *0.04 and 0.07 for nrDNA and cpDNA sequences, followed by a secondary influence of the Wanglou River, separating SE and SW clades with* Nm = *0.10 and 0.07 for nrDNA and cpDNA sequences, then the third influence of the upper Changhua River dividing NW and SE clades with* Nm = *0.40 and 0.41 for nrDNA and cpDNA sequences (Figure 5, 90% bootstrap). Notably, the Nansheng River splits nrITS clade SE into two subclades (BS below 80%, Figure 5A). Besides, according to the BARRIER analysis, the isolation magnitudes were proportional to the size of the rivers; the lower Changhua River features the greatest impact, possibly owing to its much larger width (1660 m, vs only 300 m of the upper Changhua River and 160 m of the Wanglou River), and bigger discharge volume.*

4.2 The role of rivers on evolutionary history of P. heterotricha

Our phylogenetic trees and dating analyses convincingly indicate that the closest phylogenetic relationship of P. heterotricha *is*P. pteropoda *(mainly distributed in the South of mainland China), and the colonization event that gave rise to* P. heterotricha*occurred at* c. *0.83 Myr, approximately coinciding with the formation of the Qiongzhou Strait (Zhao et al. , 2007).*

The analyses of the ribotypes and chlorotypes converge in suggesting a widespread pristine distribution of P. heterotricha *in the south-central mountain system of Hainan Island. At* c . *0.83 Myr (Figure 3), two vicariance events gave rise to the genetic split of the species first in two clades (SW and the rest), and later in three clades (SW, NW and SE, Figure 2, 3, S3). Meanwhile, The barriers represented by the Changhua and Wanglou rivers are very old, as their origins date back to Hercynian-Indosinian ages (236-257 Myr) and Late Yanshanian ages (*c. *99 Myr), respectively (Wang et al. , 2015), long before the estimated differentiation within* P. heterotricha *and in other Hainan endemic Gesneriaceae (Ling et al. , 2017b). Thus, gene flow restrictions induced by these rivers may have affected many species of the biota of Hainan Island throughout long geological periods.*

*Cogent with genetic isolation between clade SW and other two clades (at*c. *0.83 Myr) and between clades NW and SW (starting at* c.*0.48 Myr), one possibility to explain the high differentiation of the three current lineages of* P. heterotricha *is limited gene flow after the colonization of the south-central mountain (feasibly triggered by the tropical monsoon, Ling et al. , 2017a, b). The small brown and fusiform shaped seeds intimate weak dispersal capabilities either by anemochory (i.e. wind-dispersal) or zoochory (i.e. animal-mediated dispersal), deep and wide rivers may enhance barriers of seeds dispersal. Furthermore, at the estimated time of isolation between clades the water discharge of Changhua River and Wanglou River was probably greater, consistent with the increased precipitation regime that prevailed in the area in the early Holocene (Zheng et al. , 2004). Both factors likely contributed to the strengthening of the earlier genetic barriers and shaped the observed inter-regional genetic differentiation.*

*This scenario is not incompatible, however, with the possibility of multiple colonization events from the mainland to Hainan (the distance from the mainland is quite low, some 20 km across the straits of Qiongzhou), followed by secondary contact and further dispersal and isolation to originate the three genetic lineages. This would also help explain the high genetic variation levels and structuring detected in*P. heterotricha *. Similar processes related to low distances to the mainland and the geological ontogeny of the islands have been suggested to be frequent in other islands and archipelagos with high levels of endemicity (Caujapé-Castells et al., 2017; Stuessy et al. , 2014). Finally, the possibility of independent colonization events to the three areas of current distribution of* P. heterotricha *is not supported by the mismatch distribution analysis. However, three clades of* P. heterotricha *had no observable morphological differentiation within south-central mountain system, which may indicate the species could be at an early diversification stage.*

4.3 The drivers of biodiversification in Hainan Island

As one of world-wide biodiversity hotspot, the richest biotic assembly were shaped in south-central mountains of Hainan Island. Apart from island isolation and monsoon climate factors, the phylogeographical patterns of multiple clades of Gesneriaceae were driven by Changhua River (Li et al., 2020; Ling et al., 2020a), which blocked gene flow between populations, and even facilitated significant distinctive climates on different sides (Xing et al., 2012). Thus, differ from uplift-driven diversification in the Hengduan Mountains (Xing & Ree, 2017), current plant diversity in South America under Andean orogeny (Luebert & Weigend, 2014), the high biodiversity and endemism may be caused by the positive isolation effect of Changhua and Wanglou Rivers.

However, Changhua River has potentially negative effects on landscape pattern and ecosystem integrity of Hainan Tropical Rainforest National Park by declining connection degree and increasing landscape fragmentation. The further habitat isolation and fragmentation caused by the expressway G9811 probably possess negative ecological effects in future. So, the ecological corridor should be constructed across Changhua River and expressway to lower ecological risk.

5 CONCLUSIONS

Our investigation revealed three well supported genetic clades in the Hainan island endemic plant P. heterotricha *, and proposed hypotheses to construe the phylogeographic patterns detected (Figure 2 and 3). The genetic results highlight for the first time the critical role of riverine isolation caused by the Changhua and Wanglou Rivers in the patterns of intraspecific evolution of plant populations on Hainan Island. However, such barrier effects for the speciation mechanism of this island-endemic herb and other similar plants are still in need of further illumination, especially by reproductive studies, and enhanced mainland sampling. Both are important to construe the origins of the species' high current genetic diversity.*

Importantly, the three groups of populations detected are genetically quite distinct, which calls for their independent management in any conservation strategy, in order to avoid disrupting their current genetic structure and their prospects of future evolution.

ACKNOWLEDGMENTS

This work was funded by the Innovative Team Program of Hainan Natural Science Foundation (2018CXTD334), National Natural Science Foundation of China (31670230 and 41871041). We thank Zhe

Zhang, Ke Tan for field sampling and data analyses, staffs from Mt. Bawang and Yingge National Nature Reserve for providing various helps in the field.

CONFLICT OF INTEREST

We have no conflicts of interest to declare.

AUTHOR CONTRIBUTION

Shaojun Ling: *Data curation (lead); Formal analysis (lead); Investigation (equal); Writing-original draft (lead).* ***Juli Caujapé-Castells:*** *Writing-review & editing (supporting).* ***Liang Tang:*** *Conceptualization (equal); Writing-review & editing (supporting).* ***Mingxun Ren:*** *Investigation (equal); Conceptualization (equal); Funding acquisition (lead); Project administration (lead); Supervision (lead); Writing-review & editing (supporting).*

DATA AVAILABILITY STATEMENT

*All newly acquired sequences have been deposited in GenBank (http://www.ncbi.nlm.nih.gov) under accession numbers MW165394-MW165405 (ITS1/2), MW196628-MW196646 (*trn *L*-trn *F), MZ391871, MZ479364-MZ479381 (*ycf *1b).*

REFERENCES

*Akaike, H. (1981). Likelihood of a model and information criteria.*Journal of Econometrics*, 16(1), 3–14. https://doi.org/10.1016/0304-4076(81)90071-3 Antonelli, A., Nylander, J. A. A., Persson, C., & Sanmatín, L. (2009). Tracing impact of the Andean uplift in Neotropical plant evolution.*Proceeding of the National Academy of Sciences of the United States of America*, 106(24), 9749–9754. https://doi.org/10.1073/pnas.0811421106 Bouckaert, R., Heled, J., Kühnert, D., Vaughan, T., Wu, C. H., Xie, D., Suchard, M. A., Rambaut, A., & Drummond, A. J. (2014). BEAST 2: A Software Platform for Bayesian Evolutionary Analysis.* PLoS Computational Biology*, 10(4), e1003537. https://doi.org/10.1371/journal.pcbi.1003537 Buso, G. S. C., Rangel, P. H., & Ferreira, M. E. (1998). Analysis of genetic variability of South American wild rice populations (*Oryza glumaepatula*) with isozymes and RAPD markers.* Molecular Ecology*, 7(1), 107–117. https://doi.org/10.1046/j.1365-294x.1998.00321.x Crimmins, T. M., Crimmins, M. A., & Bertelsen, C. D. (2011). Onset of summer flowering in a 'Sky Island' is driven by monsoon moisture.*New Phytologist*, 191(2), 468–479. https://doi.org/10.1111/j.1469-8137.2011.03705.x Caujapé-Castells, J., García-Verdugo, C., Marrero-Rodríguez, A., Fernández-Palacios J. M., Crawford, D. J., & Mort, M. E. (2017). Island ontogenies, syngameons, and the origins of genetic diversity in the Canarian flora.* Perspectives in Plant Evolution, Ecology and Systematics*, 27(2017), 9–22. https://doi.org/10.1016/j.ppees.2017.03.003 Demenou, B. B., Piñeiro, R., & Hardy, O. J. (2016). Origin and history of the Dahomey Gap separating West and Central African rain forests: insights from the phylogeography of the legume tree* Distemonanthus benthamianus*. Journal of Biogeography, 43(5), 1020–1031. https://doi.org/10.1111/jbi.12688 Doyle, J. J., & Doyle, J. L. (1987). A rapid DNA isolation method for small quantities of fresh tissues.* Phytochemical Bulletin, Botanical Society of America*, 19(1), 11–15. Dong, W. P., Xu, C., Li, C. H., Sun, J. H., Zuo, Y. J., Shi, S., Cheng, T., Guo, J. J., & Zhou, S. L. (2015).* ycf*1, the most promising plastid DNA barcode of land plants.* Scientific Reports*, 5(1), 8348. https://doi.org/10.1038/srep08348 Drummond, A. J., Suchard, M. A., Xie, D., & Rambaut, A. (2012). Bayesian Phylogenetics with BEAUti and the BEAST 1.7.* Molecular Biology and Evolution*, 29(8), 1969–1973. https://doi.org/10.1093/molbev/mss075 Earl, D. A., & vonHoldt, B. M. (2012). STRUCTURE HARVESTER: a website and program for visualizing STRUCTURE output and implementing the Evanno method.* Conservation Genetics Resources*, 4(2), 359–361. https://doi.org/10.1007/s12686-011-9548-7 Evanno, G. S., Regnaut, S., & Goudet, J. (2005). Detecting the number of clusters of individuals using the software STRUCTURE: a simulation study.* Molecular Ecology*, 14(8), 2611–2620. https://doi.org/10.1111/j.1365-294X.2005.02553.x Francisco-Ortega, J., Wang, Z. S., Wang, F. G., Xing, F. W., Liu, H., Xu, H., Xu, W. X., Luo, Y. B., Song, X. Q., Gale, S., Boufford, D. E., Maunder, M., & An, S Q. (2010a). Seed Plant Endemism on Hainan Island: A Framework for Conservation Actions.* The Botanical Review*, 76, 346–*

376. https://doi.org/10.1007/s12229-010-9055-7 Francisco-Ortega, J., Wang, F. G., Wang, Z. S., Xing, F. W., Liu, H., Xu, H., Xu, W. X., Luo, Y. B., Song, X. Q., Gale, S., Boufford, D. E., Maunder, M., & An, S. Q. (2010b). Endemic Seed Plant Species from Hainan Island: A Checklist. The Botanical Review*, 76, 295–345. https://doi.org/10.1007/s12229-010-9054-8 Fu, Y. X. (1997). Statistical tests of neutrality of mutations against population growth, hitchhiking and background selection.*Genetics*, 147(2), 915–925. Gao, Y., Ai, B., Kong, H. H., Kang, M., & Huang, H. W. (2015). Geographical pattern of isolation and diversification in karst habitat islands: a case study in the* Primulina eburnea *complex.*Journal of Biogeography*, 42(11), 2131–2144. https://doi.org/10.1111/jbi.12576 Hall, T. A. (1999). BioEdit: A User-friendly Biological Sequence Alignment Editor and Analysis Program for Windows 95/98/NT.*Nucleic Acids Symposium Series*, 41, 95–98. https://doi.org/10.14601/Phytopathol_Mediterr-14998u1.29 Kumar, S., Nei, M., Dudley, J., & Tamura, K. (2008). MEGA: A biologist-centric software for evolutionary analysis of DNA and protein sequences.* Briefings in Bioinformatics*, 9(4), 299–306. https://doi.org/10.1093/bib/bbn017 Li, Z. Y., & Wang, Y. Z. (2005).* Plants of Gesneriaceae in China*. Henan Science and Technology Publishing House. Li, Y., Zhai, S. N., Qiu, Y. X., Guo, Y. P., Ge, X. J., & Comes, H. P. (2011). Glacial survival east and west of the 'Mekong–Salween Divide' in the Himalaya–Hengduan Mountains region as revealed by AFLPs and cpDNA sequence variation in* Sinopodophyllum hexandrum*(Berberidaceae).* Molecular Phylogenetics and Evolution*, 59(2), 412–424. https://doi.org/10.1016/j.ympev.2011.01.009 Li, G., Ling, S. J., Chen, W. F., Ren, M. X., & Tang, L. (2020). Effects of geographic isolation caused by Changhua River on genetic diversity of Hainan-endemic* Metapetrocosmea peltata*(Gesneriaceae).* Guihaia*, 40(10), 1505–1513. http://kns.cnki.net/kcms/detail/45.1134.q.20190128.1718.006.html Ling, S. J. (2017). "Regional life tree" of Gesneriaceae in Hainan Island and the differentiation of an endemic species-*Chirita heterotricha *driven by Changhuajiang River. Master's Degree dissertation, Hainan University. Ling, S. J., Meng, Q. W., Tang, L., & Ren, M. X. (2017a). Pollination syndromes of Chinese Gesneriaceae: a comparative study between Hainan Island and neighboring regions.* The Botanical Review*, 83, 59–73. https://doi.org/10.1007/s12229-017-9181-6 Ling, S. J., Meng, Q. W., Tang, L., & Ren, M. X. (2017b). Gesneriaceae on Hainan Island: distribution patterns and phylogenetic relationships.*Biodiversity Science*, 25(8), 807–815. https://doi.org/10.17520/biods.2016360 Ling, S. J., Qin, X. T., Song, X. Q., Zhang, L. N., & Ren, M. X. (2020a). Genetic delimitation of* Oreocharis *species from Hainan Island.* PhytoKeys*, 157, 59–81. https://doi.org/10.3897/phytokeys.157.32427 Ling, S. J., Guan, S. P., Wen, F., Shui, Y. M., & Ren, M.X. (2020b).*Oreocharis jasminina *(Gesneriaceae), a new species from mountain tops in Hainan Island, South China.* PhytoKeys*, 157, 121–135. https://doi.org/10.3897/phytokeys.157.50246 Liu, Y. F., Wang, Y., Huang, H. W. (2009). Species-level phylogeographical history of* Myricaria *plants in the mountain ranges of western China and the origin of* M. laxiflora *in the Three Gorges mountain region.* Molecular Ecology*, 18(12), 2700–2712. https://doi.org/10.1111/j.1365-294X.2009.04214.x Liu, J., Möller, M., Provan, J., Gao, L. M., Poudel, R. C., & Li, D. Z. (2013). Geological and ecological factors drive cryptic speciation of yews in a biodiversity hotspot.* New Phytologist*, 199(4), 1093–1108. https://doi.org/10.1111/nph.12336 Luebert, F., & Weigend, M. (2014). Phylogenetic insights into Andean plant diversification.* Frontiers in Ecology and Evolution*, 2(192), 1–17. https://doi.org/10.3389/fevo.2014.00027 MacArthur, R. H., & Wilson, E. O. (1967).* The Theory of Island Biogeography*. Princeton University Press. Mantel, N. (1967). The detection of disease clustering and a generalized regression approach.* Cancer Research*, 27(2), 209–220. Manni, F., Guérard, E., & Heyer, E. (2004). Geographic Patterns of (Genetic, Morphologic, Linguistic) Variation: How Barriers Can Be Detected by Using Monmonier's Algorithm.* Human Biology*, 76(2), 173–190. https://doi.org/10.1353/hub.2004.0034 Myers, N., Mittermeier, R. A., Mittermeier, C. G., da Fonseca, G. A., & Kent, J. (2000). Biodiversity hotspots for conservation priorities.*Nature*, 403(6772), 853–858. https://doi.org/10.1038/35002501 Nei, M. (1973). Analysis of Gene Diversity in Subdivided Populations.*Proceedings of the National Academy of Sciences of the United States of America*, 70(12), 3321–3323. https://doi.org/10.1073/pnas.70.12.3321 Nylander, J. A. A. (2004).* MrModeltest v2. Program distributed by the author*. Uppsala: Evolutionary Biology Centre, Uppsala University. Pennington, R. T., Lavin, M., Särkinen, T., Lewis, G. P., Klitgaard, B. B., & Hughes, C. E. (2010). Contrasting plant diversification histories within the Andean biodiversity hotspot.* Proceedings of the National Academy of Sciences of the United States of America*, 107(31), 13783–13787. htt-*

*ps://doi.org/10.1073/pnas.1001317107 Peakall, R., & Smouse, P. E. (2012). GenAlEx 6.5: genetic analysis in Excel. Population genetic software for teaching and research-an update.*Bioinformatics*, 28(19), 2537–2539. https://doi.org/10.1093/bioinformatics/bts460 Pons, O., & Petit, R. J. (1996). Measuring and testing genetic differentiation with ordered versus unordered alleles.* Genetics*, 144(3), 1237–1245. Rambaut, A., & Drummond, A. J. (2007). Tracer v1.5. Available at: http://beast.bio.ed.ac.uk/Tracer. Rambaut, A. (2009). Figtree v.1.4.2. Available at: http://tree.bio.ed.ac.uk/software /figtree. Robin, V. V., Vishnudas, C. K., Gupta, P., & Ramakrishnan, U. (2015). Deep and wide valleys drive nested phylogeographic patterns across a montane bird community.* Proceedings of the Royal Society B: Biological Sciences*, 282(1810), 20150861. https://doi.org/10.1098/rspb.2015.0861 Ronquist, F., Teslenko, M., van der Mark, P., Ayres, D. L., Darling, A., Höhna, S., Larget, B., Liu, L., Suchard, M. A., & Huelsenbeck, J. P. (2012). MrBayes 3.2: Efficient Bayesian Phylogenetic Inference and Model Choice Across a Large Model Space.* Systematic Biology*, 61(3), 539–542. Rozas, J., Ferrer-Mata, A., Sánchez-DelBarrio, J. C., Guirao-Rico, S., Librado, P., Ramos-Onsins, S. E., & Sánchez-Gracia, A. (2017). DnaSP 6: DNA Sequence Polymorphism Analysis of Large Data Sets.* Molecular Biology and Evolution*, 34(12), 3299–3302. https://doi.org/10.1093/molbev/msx248 Slatkin, M. (1985). Gene flow in natural populations.* Annual Review of Ecology and Systematics*, 16, 393–430. Stuessy, T. F., Takayama, K., López-Sepúlveda, P., & Crawford, D. J. (2014). Interpretation of patterns of genetic variation in endemic plant species of oceanic islands.* Botanical Journal of the Linnean Society*, 174(3), 276–288. https://doi.org/10.1111/boj.12088 Swofford, D. L. (2002). PAUP*: Phylogenetic Analysis Using Parsimony, Version 4.0b10. Sunderland, MA: Sinauer. Taberlet, P., Gielly, L., Pautou, G., Bouvet, J. (1991) Universal primers for amplification of three non-coding regions of chloroplast DNA.* Plant Molecular Biology*, 17(5), 1105–1109. https://doi.org/10.1007/BF00037152 Tajima, F. (1989). Statistical method for testing the neutral mutation hypothesis by DNA polymorphism.* Genetics*, 123(3), 585–595. Tan, K., Malabrigo, P. L., & Ren, M. X. (2020). Origin and evolution of biodiversity hotspots in Southeast Asia.* Acta Ecologica Sinica*, 40(11), 3866–3877. https://doi.org/10.5846/stxb201904160762 Vaidya, G., Lohman, D. J., & Meier, R. (2011). SequenceMatrix: concatenation software for the fast assembly of multi-gene datasets with character set and codon information.* Cladistics*, 27(2), 171–180. https://doi.org/10.1111/j.1096-0031.2010.00329.x Wang, C., Liang, X. Q., Zhou, Y., Fu, J. G., Jiang, Y., Dong, C. G., Xie, Y. H., Tong, C. X., Pei, J. X., & Liu, P. (2015). Construction of age frequencies of provenances on the eastern side of the Yinggehai Basin: Studies of LA-ICP-MS U-Pb ages of detrital zircons from six modern rivers, western Hainan, China.* Earth Science Frontiers*, 22(4), 277–289. https://doi.org/10.13745/j.esf.2015.04.028 Wei, Y. G., Zhong, S. H., Wen, H. Q. (2004). Studies of the flora and ecology Gesneriaceae in Guangxi Province.* Acta Botanica Yunnanica*, 26, 173–182. Wei, Y. G. (2010).* Gesneriaceae of South China*. Guangxi Science and Technology Publishing House. White, T. J., Bruns, T. D., Lee, S. B., & Taylor, J. (1990). Amplification and Direct Sequencing of Fungal Ribosomal RNA Genes for Phylogenetics.* PCR Protocols*, 1990, 315–322. Xing, F. W., Zhou, J. S., Wang, F. G., Zeng, Q. W., Yi, Q. F., & Liu, D. M. (2012).* Inventory of Plant Species Diversity of Hainan*. Huazhong University of Science & Technology Press. Xing, Y. W., & Ree, J. S. (2017). Uplift-driven diversification in the Hengduan Mountains, a temperate biodiversity hotspot.* Proceeding of the National Academy of Sciences of the United States of America*, 114(17), E3444–E3451. https://doi.org/10.1073/pnas.1616063114 Yang, X. B. (2013).* Flora of Hainan*. Science Press. Yu, S. X., Zang, R. G., & Jiang, Y. X. (2001). Spatial analysis of species diversity in the tropical vegetations along the vertical belt at Bawangling Nature Reserve, Hainan Island.* Acta Ecologica Sinica*, 9, 1438–1443. Yu, Y., Harris, A. J., & He, X. (2010). S-DIVA (Statistical Dispersal-Vicariance Analysis): a tool for inferring biogeographic histories.* Molecular Phylogenetics and Evolution*, 56(2), 848–850. https://doi.org/10.1016/j.ympev.2010.04.011 Zhao, H. T., Wang, L. R., & Yuan, J. Y. (2007). Origin and time of Qiongzhou Stait.* Marine Geology & Quaternary Geology*, 27, 33–40. Zheng, Z., Deng, Y., Zhang, H., Yu, R. C., & Chen, Z. X. (2004). Holocene environmental changes in the tropical and subtropical areas of the South China and the relation to human activities.* Quaternary Sciences*, 24(4), 387–393. https://doi.org/10.3321/j.issn:1001-7410.2004.04.003 Zhong, Y. F., Zhang, Z., Song, X. Q., & Zhou, Z. D. (2014). Pollination biology of* Impatiens hainanensis *(Balsaminaceae) populations at different altitudes.* Biodiversity Science*, 22(4), 467–475. https://doi.org/10.3724/SP.J.1003.2014.13243*

TABLE 1 *Sampling information, haplotype information, haplotype diversity within-population (Hd) of* P. heterotricha*, pri*

Code	
BW	
YJ	
EX	
WX	
YG	
WZ	
QX	
XA	
QL	
JF	

TABLE 2 *Sequences of the primers used for genetic studies of* P. heterotricha*, and main descriptors of the obtained fragm*

DNA fragment	
ITS1/2	
trn*L*-trn*F*	
ycf*1b*	
trn*L*-trn*F and* ycf*1b*	

TABLE 3 *Pairwise comparisons of* Fst *estimates (above diagonal) and deduced* Nm *values (below diagonal) between popul*

nrITS	
BW	
YJ	
EX	
WX	
YG	
WZ	
QX	
XA	
QL	
JF	
cpDNA	
BW	
YJ	
EX	
WX	
YG	
WZ	
QX	
XA	
QL	
JF	

TABLE 4 *AMOVA analysis of* P. heterotricha *based on nrITS and cpDNA sequence data. **,* P < *0.001.*

nrITS	
Among regions	*3*
Among populations within regions	*6*
Within populations	*207*
Total	*216*
cpDNA	
Among regions	*3*
Among populations within regions	*6*
Within populations	*207*
Total	*216*

TABLE 4 *A*

Degree of free

Figure legends:

FIGURE 1 *Sampling sites and geographic distribution of the 12 ribotypes (A) and 19 chlorotypes (B) found in 10 populations of* Primulina heterotricha *from Hainan Island.*

FIGURE 2 *(A) Molecular phylogeny and (B) network of the 12 ribotypes from* Primulina heterotricha *based on nrITS data, numbers on the branches showed the Posterior probability (PP)/Bootstrap value (BS). The relative sizes of the circles in the network are proportional to the ribotype frequencies.* $'vicarianceeventsdetectedbyS-DIVA.Thedashedlinesrepresenttheisolationoftworiversin HainanIsland, andthesizeofdashedlineswascorrespondenttoth$

FIGURE 3 *(A) Chronogram for 19 chlorotypes from* Primulina heterotricha *and outgroup based on combined* trn *L*-trn *F and*ycf *1b data, analysed using a relaxed molecular clock approach, posterior probabilities (PP) are showed above branches. (B) Network of 19 chlorotypes from* Primulina heterotricha *based on combined*trn *L*-trn *F and* ycf *1b data, the relative sizes of the circles in the network are proportional to the chlorotypes frequencies, and missing chlorotypes are represented by small black spot.* $'vicarianceeventsdetectedbyS-DIVA.Thedashedlinesrepresenttheisolationoftworiversin HainanIsland, andthesizeofdashedlineswascorrespondenttoth$

FIGURE 4 *Histogram of the STRUCTURE for all individuals at K=3 based on ITS1/2, the size of arrow lines were correspondent to the isolation level of rivers.*

FIGURE 5 *Results of Barrier analysis based on the (A) ITS1/2 and (B) combined* trn *L*-trn *F and* ycf *1b, indicating the spatial separation of* Primulina heterotricha *populations, Delaunay triangulation (black lines) and inferred barriers (red, green and blue lines) separating the different original regions which showing the geographic location of the genetic barrier, black spots represent corresponding population location. NW, northwest of Changhua R., including populations BW, YJ, EX, WX and YG; SE, southeast of Changhua R., including populations WZ, QX, XA and QL; SW, southwest of Changhua R., including population JF.*

FIGURE S1 *The results graph of the relationship between genetic and geographic distance for 10 populations based on the (A) nrITS and (B) cpDNA.*

FIGURE S2 *Bayesian inference analysis of nrITS for the determination of the most likely number of genetic clusters (K).*

FIGURE S3 *Graphical output from S-DIVA. (A) Graphical results of ancestral distributions at each node of the phylogeny of chlorotypes from* P. heterotricha *obtained by S-DIVA. Alternative ancestral ranges of nodes I and II (with frequency of occurrence) are shown in pie chart form. Posterior probabilities (PP) are indicated by the sides of pie charts. (B) Colour blocks to possible ancestral ranges at different nodes. NW, northwest of Changhua R., including populations BW, YJ, EX, WX and YG; SE, southeast of Changhua R., including populations WZ, QX, XA and QL; SW, southwest of Changhua R., including population JF.* $'possiblevicarianceeventsdetectedbyS-DIVA.$

FIGURE S4 *Mismatch distribution analysis plots across all populations of (A) nrITS and (E) cpDNA and clade NW region of (B) nrITS and (F) cpDNA, clade SE region of (C) nrITS and (G) cpDNA, clade SW region of (D) nrITS and (H) cpDNA.*

FIGURE 1

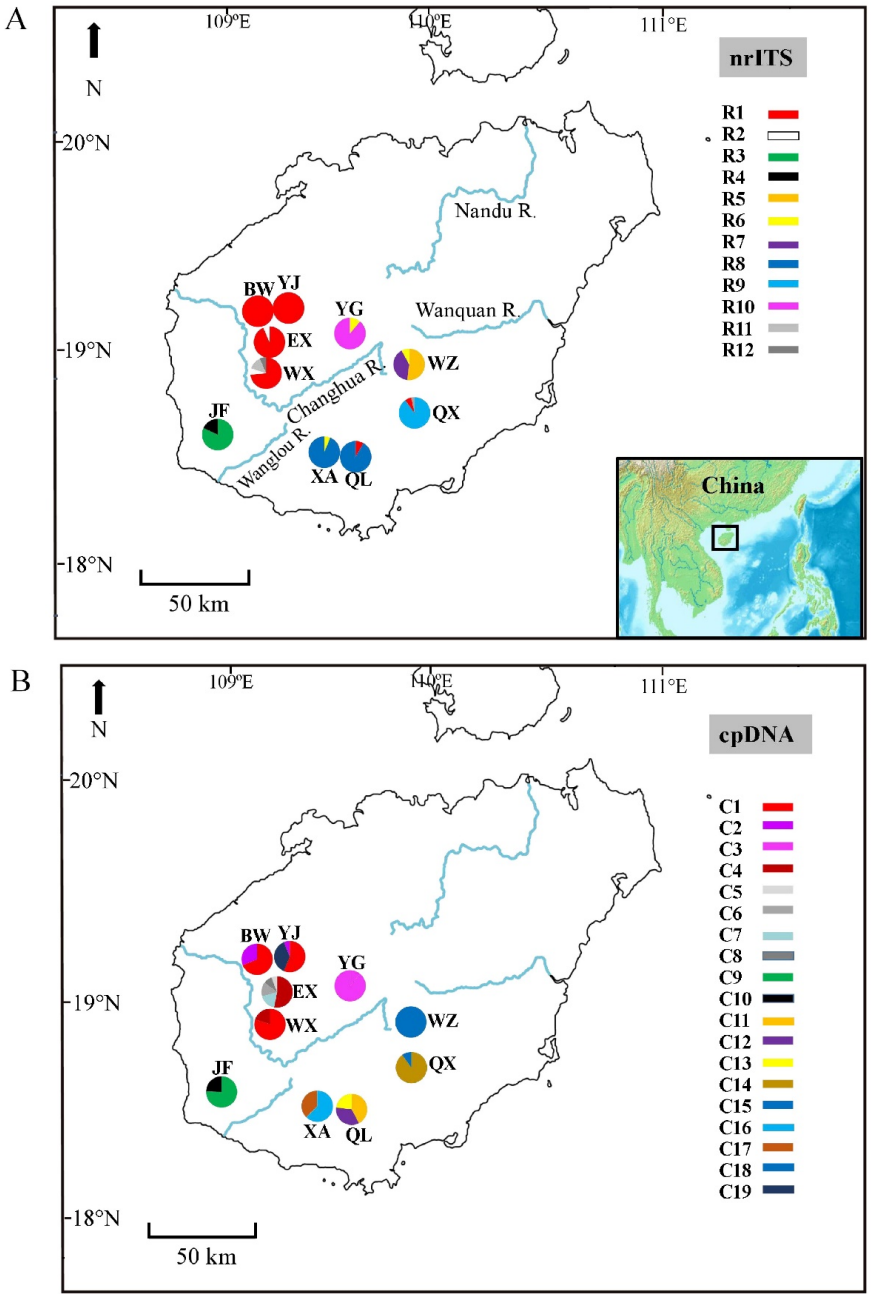

FIGURE 2

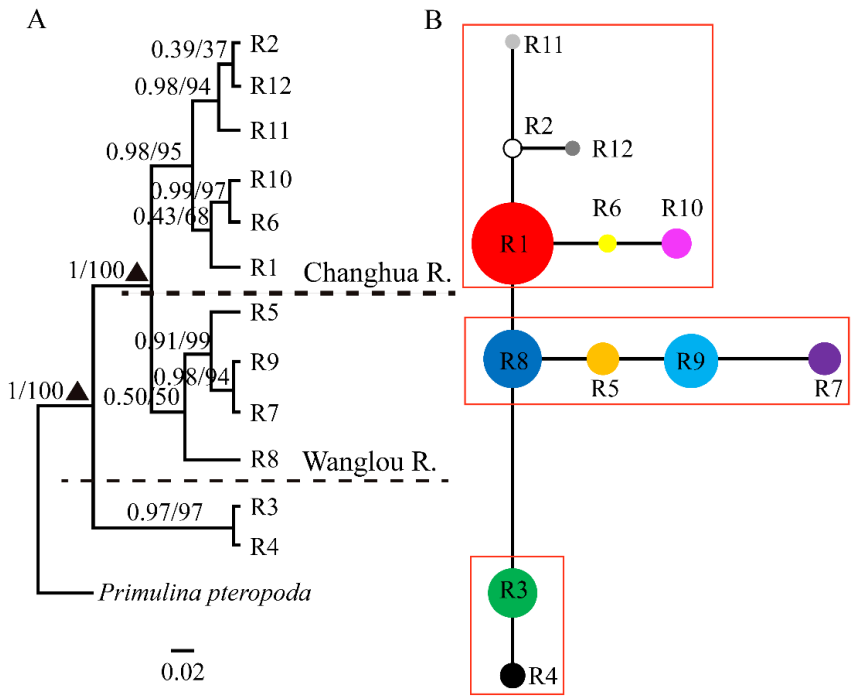

FIGURE 3

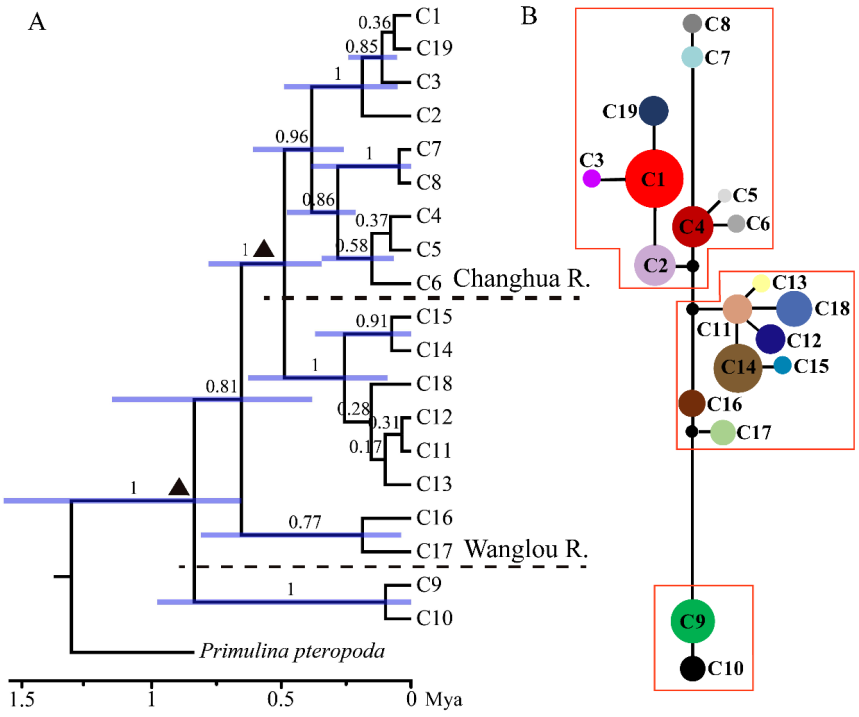

FIGURE 4

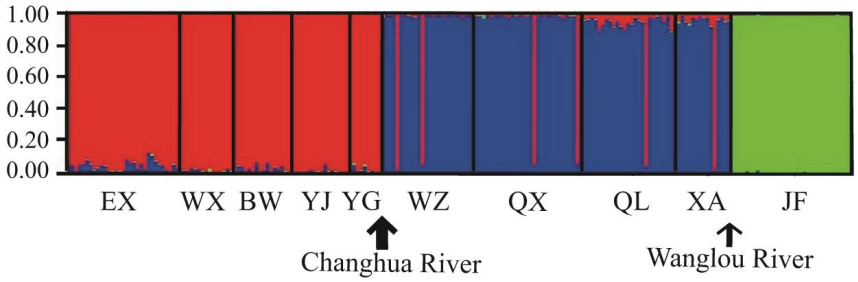

FIGURE 5

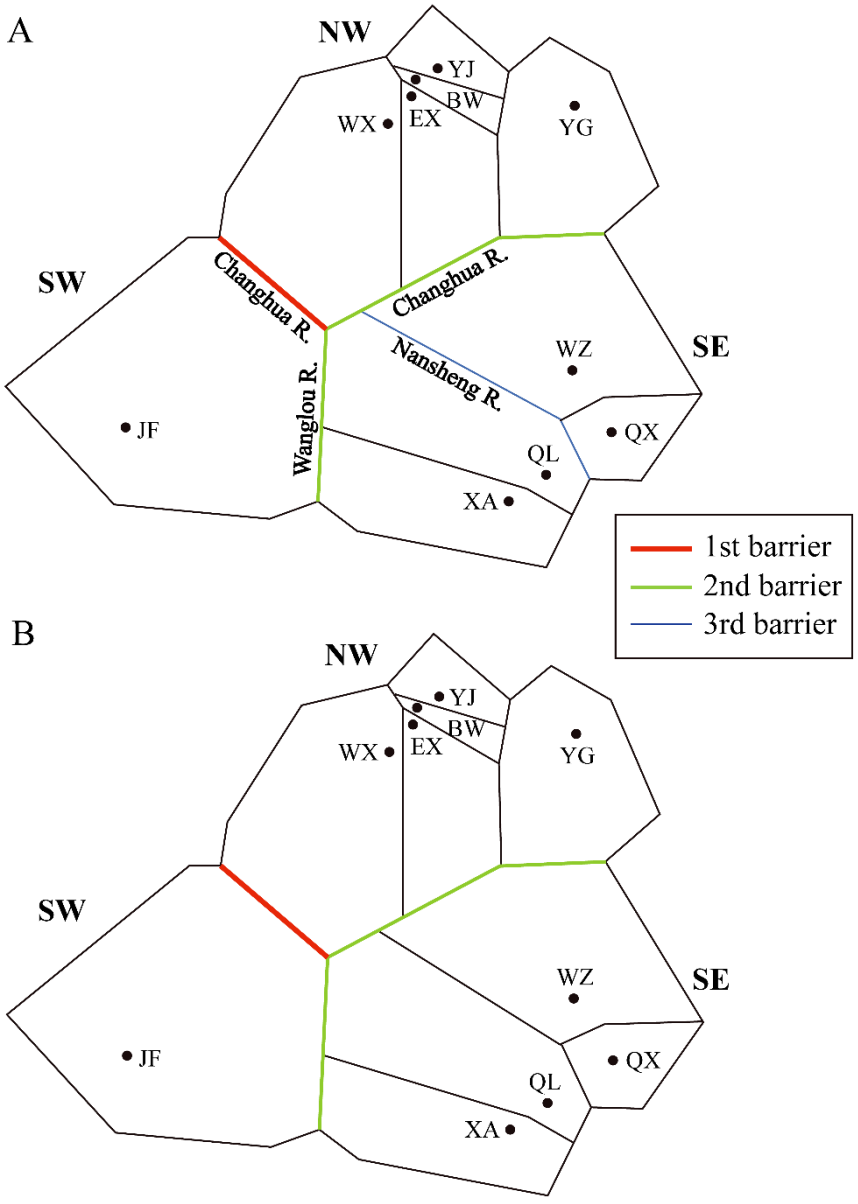

FIGURE S1

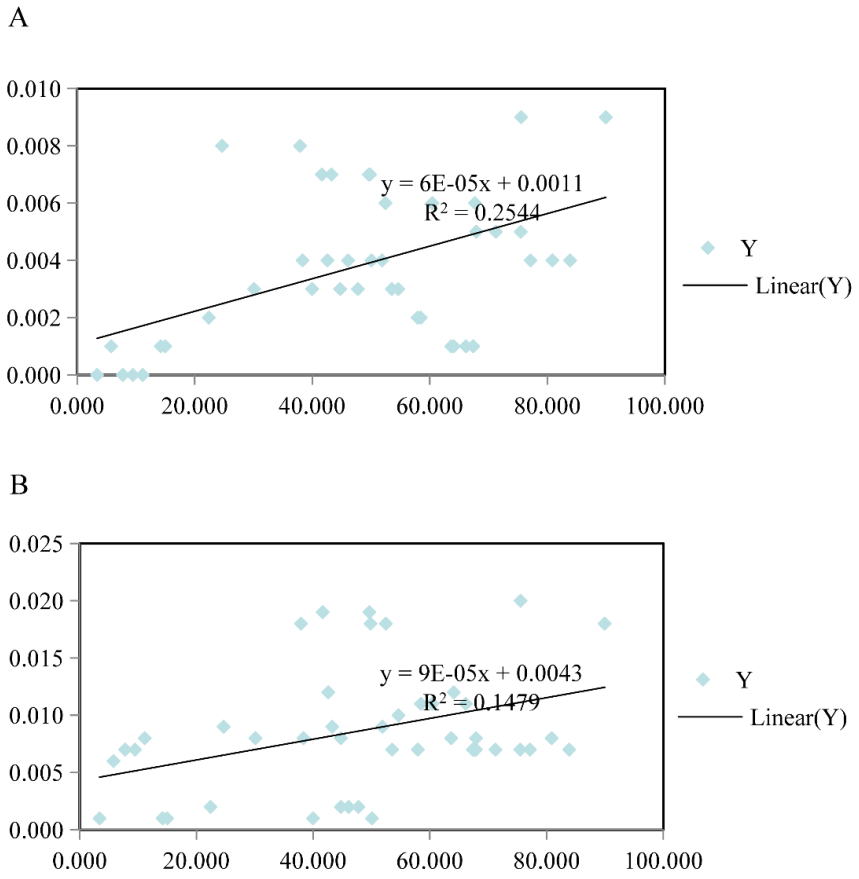

FIGURE S2

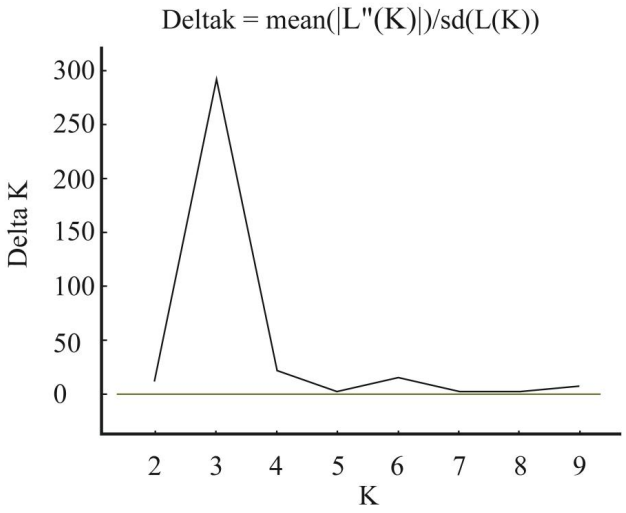

FIGURE S3

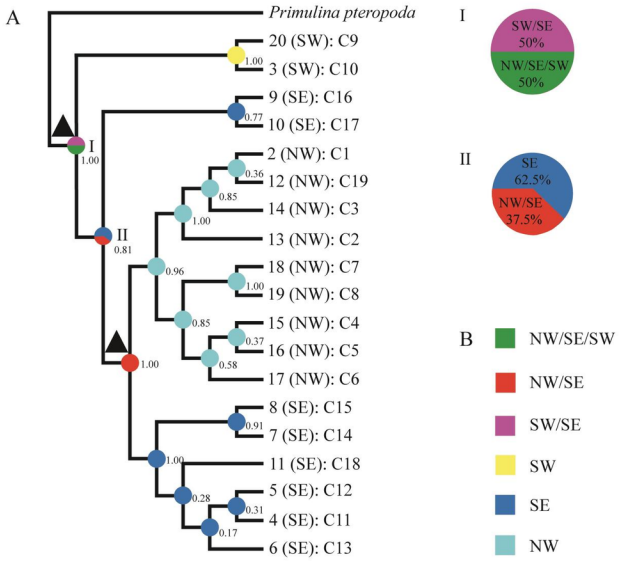

FIGURE S4